



ORIGINAL ARTICLE

Single-cell biology uncovers apoptotic cell death and its spatial organization as a potential modifier of tumor diversity in HCC

Subreen A. Khatib^{1,2} | Lichun Ma¹ | Hien Dang^{1,3} | Marshonna Forgues¹ | Joon-Yong Chung⁴  | Kris Ylaya⁴ | Stephen M. Hewitt⁴ | Jittporn Chaisaingmongkol^{5,6} | Mathuros Rucchirawat^{5,6} | Xin Wei Wang^{1,7} 

¹Laboratory of Human Carcinogenesis, Center for Cancer Research, National Cancer Institute, Bethesda, Maryland, USA

²Department of Tumor Biology, Lombardi Comprehensive Cancer Center, Georgetown University Medical Center, Washington, DC, USA

³Division of Surgery, Thomas Jefferson University, Philadelphia, Pennsylvania, USA

⁴Laboratory of Pathology, Center for Cancer Research, National Cancer Institute, Bethesda, Maryland, USA

⁵Laboratory of Chemical Carcinogenesis, Chulabhorn Research Institute, Bangkok, Thailand

⁶Center of Excellence on Environmental Health and Toxicology, Office of the Higher Education Commission, Ministry of Education, Bangkok, Thailand

⁷Liver Cancer Program, Center for Cancer Research, National Cancer Institute, Bethesda, Maryland, USA

Correspondence

Xin Wei Wang, Laboratory of Human Carcinogenesis and Liver Cancer Program, Center for Cancer Research, National Cancer Institute, NIH, Bethesda, MD 20892, USA.
Email: xw3u@nih.gov

Funding information

Supported by the intramural research program of the Center for Cancer Research, National Cancer Institute (Z01 BC 010877 and Z01 BC 010876)

Abstract

Background and Aims: HCC is a highly aggressive and heterogeneous cancer type with limited treatment options. Identifying drivers of tumor heterogeneity may lead to better therapeutic options and favorable patient outcomes. We investigated whether apoptotic cell death and its spatial architecture is linked to tumor molecular heterogeneity using single-cell *in situ* hybridization analysis.

Approach and Results: We analyzed 254 tumor samples from two HCC cohorts using tissue microarrays. We developed a mathematical model to quantify cellular diversity among HCC samples using two tumor markers, cyclin-dependent kinase inhibitor 3 and protein regulator of cytokinesis 1 as surrogates for heterogeneity and caspase 3 (*CASP3*) as an apoptotic cell death marker. We further explored the impact of potential dying-cell hubs on tumor cell diversity and patient outcome by density contour mapping and spatial proximity analysis. We also developed a selectively controlled *in vitro* model of cell death using CRISPR/CRISPR-associated 9 to determine therapy response and growth under hypoxic conditions. We found that increasing levels of *CASP3*⁺ tumor cells are associated with higher tumor diversity. Interestingly, we discovered regions of densely populated *CASP3*⁺, which we refer to as *CASP3*⁺ cell islands, in which the nearby cellular heterogeneity was found to be the greatest compared to cells farther away from these islands and that this phenomenon was associated with survival. Additionally, cell culture experiments revealed that higher levels of cell death, accompanied by increased *CASP3* expression, led to greater therapy resistance and growth under hypoxia.

Abbreviations: Cas9, CRISPR-associated 9; *CASP3*, caspase 3; CD, cell death; *CDKN3*, cyclin-dependent kinase inhibitor 3; DOX, doxycycline; HRP-C, horseradish peroxidase isozyme C; ITH, intratumoral heterogeneity; LCI, Liver Cancer Institute; MCL-1, myeloid cell leukemia 1; MOI, multiplicity of infection; *PRC1*, protein regulator of cytokinesis 1; RNAseq, RNA sequencing; sgRNA, single-guide RNA; TIGER-LC, Thailand Initiative in Genomics and Expression Research for Liver Cancer; TMA, tissue microarray.

© 2022 American Association for the Study of Liver Diseases. This article has been contributed to by US Government employees and their work is in the public domain in the USA.

Conclusions: These results are consistent with the hypothesis that increased apoptotic cell death may lead to greater tumor heterogeneity and thus worse patient outcomes.

BACKGROUND

Intratumor heterogeneity (ITH) can be classified as one of the largest clinical conundrums in treating cancer today. Defined as the genomic and phenotypic differences seen among individual cancer cells within the same tumor, ITH poses significant challenges in determining and creating molecularly targeted therapeutics. This is especially evident in liver cancer, which is the fourth deadliest cancer type in the world, amounting to over 782,000 of deaths per year with 5-year survival rates at a dismal 18%.^[1,2] HCC, the most common form of liver cancer, contains vast levels of heterogeneity with numerous cancer mutations but no dominant drivers, making current standard-of-care practices limited in improving patient outcomes.^[3] Identifying plausible mechanisms of tumor heterogeneity can lead us toward developing better approaches to combat cancer's destructive power and therapeutically exploit its diversity. Recently, we tested the idea of cell death as a contributor in promoting increased tumor diversity.^[4] Consistently, we found that the degree of cell death in each tumor measured by an apoptotic index is positively correlated with the Tumor Shannon Entropy Index (a metric that measures cellular diversity in individual cancer cells) in seven cancer types with available single-cell RNA-sequencing (RNAseq) data. Moreover, when patients were stratified in high versus low expression on the apoptotic index, those in the high-risk category had worse overall survival compared to those in the low-risk group.^[4]

Here, using single-cell *in situ* hybridization (RNAScope technology), we aimed to validate our previous findings of increased apoptotic cell death in promoting tumor diversity using patient tumor tissue microarrays stained with an apoptotic marker and two other markers to model the state of heterogeneity of the tumor and correlate with patient outcome. We conducted a robust computational approach to identify two markers of heterogeneity, cyclin-dependent kinase inhibitor 3 (*CDKN3*), a gene involved in cell cycle regulation, and protein regulator of cytokinesis 1 (*PRC1*), a gene involved in mitosis that can be used for tissue staining. We further analyzed the spatial relationship between caspase 3–positive (*CASP3*⁺) cells as a surrogate for dying cells and the nearby cellular diversity. Lastly, we developed an *in vitro* CRISPR/CRISPR-associated 9 (Cas9) model to selectively induce varying levels of cell death and measure therapeutic response and growth under hypoxic conditions as an extension

of our RNAScope findings. Together, our findings provide valuable and additional insights into the plausible connection between cell death and tumor diversity and why we must adapt our method of treating cancer by incorporating the evolutionary patterns that tumor cells will undergo and their intricate spatial architecture that maintains their longevity and survival.

PATIENTS AND METHODS

Cohorts and clinical specimens

The data for the Liver Cancer Institute (LCI) was publicly downloaded from the Gene Expression Omnibus (GSE14520).^[5] The Cancer Genome Atlas Liver Hepatocellular Carcinoma data set was downloaded from Xenabrowser (<https://tcga.xenahubs.net>). The expression data for the Thailand Initiative in Genomics and Expression Research for Liver Cancer (TIGER-LC) is publicly available through from the Gene Expression Omnibus (GSE76297).^[3] The single-cell RNAseq data are publicly available through from the Gene Expression Omnibus (GSE125449).^[6] For the *in situ* hybridization staining using RNAScope, all patients with HCC from TIGER-LC were included, and a subset of the highest-quality samples from the LCI patients with HCC was selected for the tissue microarrays (TMAs). Informed consent was obtained from all patients included in both cohorts and approved by the Institutional Review Boards of the respective institutions. A description of patient characteristics is summarized in Table S1 (note: not all samples contained clinical information; therefore, the values reported may not match the total number of patients per cohort).

TMAs and RNAScope *in situ* hybridization

TMAs were constructed on 1.0-mm cores from formalin-fixed, paraffin-embedded (FFPE) tissue from our LCI and TIGER-LC cohorts. Matched tumor and nontumor tissues were used for each patient as well as internal control tissues mounted as TMAs using Superfrost PLUS Slides (Thermo Fisher Scientific; catalog no. 5951PLUS). RNAScope staining was performed on 5- μ m TMA sections using the multiplex v2 assay kit (Advanced Cell Diagnostics; catalog no. 323100). For each TMA, two extra sections were cut and mounted onto slides for positive and negative

controls. Target probes were designed for the following genes: *CASP3*, *CDKN3*, and *PRC1*. In addition, probe-Hs-PPIB (catalog no. 313901; Advanced Cell Diagnostics) and probe-dapB (catalog no. 310043; Advanced Cell Diagnostics) were used as positive and negative controls, respectively. Briefly, FFPE sections were deparaffinized using Tissue-Tek clearing agent dishes with fresh xylene and ethanol at varying concentrations. Five drops of RNAScope hydrogen peroxide were added to each deparaffinized slide and incubated for 10 min at room temperature (RT), then removed, followed by washing with distilled water. Slides were then placed into a glass cylinder containing 1× target retrieval at 99°C for 15 min, then rinsed with distilled water and placed into 100% ethanol for 3 min, followed by drying in the HybEZ Oven at 40°C (this temperature is kept constant for the remaining steps) for 5 min. Five drops of Protease Plus were added to each slide, and slides were placed back into the oven for 15 min, then washed with distilled water. Target probes were warmed for 10 min at 40°C, then mixed together, and four drops were placed onto each slide. All slides were placed into the oven for 2 h, then immediately washed with 1× wash buffer for 2 min at RT twice. Four drops of Amp 1 were added to all slides, which were placed in the oven for 30 min, followed by washing. This step was repeated for Amp 2 and Amp 3. Opal fluorophores 520 (PerkinElmer; catalog no. FP1487001KT), 570 (catalog no. FP1488001KT), and 590 (FP1497001KT) were each diluted 1:1000 separately using DMSO. The horseradish peroxidase isozyme C1 (HRP-C1) signal was developed by adding four drops of HRP-C1 to each slide, placed in the oven for 15 min, and washed twice. The diluted Opal 520 solution was added to each slide (100 μl), incubated for 30 min in the oven, and washed twice. Four drops of HRP blocker were added to each slide, and slides were incubated for 15 min and washed twice. The HRP-C2 and HRP-C3 channels were developed as stated above. Vector TrueVIEW reagent (Vector; TrueVIEW Autofluorescence Quenching Kit; catalog no. SP-8400-15) was prepared according to the manufacturer's protocol and added to each slide to reduce autofluorescence of tissue staining. Slides were counterstained with DAPI and immediately mounted using Prolong Gold antifade mounting medium (ThermoFisher Scientific; catalog no. P36934). Slides were dried overnight and imaged the next day.

TMA image acquisition and quantification using HALO

Slides were imaged using a Nikon SoRa superresolution spinning disk microscope at ×20. All imaging settings were optimized to the negative control slides, and z stacks were obtained to generate a maximum intensity z-projection for each slide. Slides were analyzed

using Indica Labs' pathology software HALO Image Analysis Platform containing the TMA, Multiplex FISH, and Spatial Modules. Single-cell probe copies were quantified, and proximity analysis between each target probe was conducted.

Computing a diversity score (Shannon Index) of the expression of heterogeneity markers *CDKN3* and *PRC1* and HALO proximity analysis

To determine the heterogeneity state of each tumor sample, *CDKN3* and *PRC1* were selected as surrogates to model heterogeneity based on the analysis described above.⁷ A Shannon Index (H_{ijt}) was used to compute a diversity score for each patient sample:

$$H_{ijt} = -\sum p_{ijt} \times \ln p_{ijt}$$

H_{ijt} is the calculated Shannon Index, p_{ij} is the proportion of selected cell population i and the total number of cells j , and t is the time point. Unique cell populations were determined by the proportions of cells that stained positive for either *CDKN3*, *PRC1*, or both as well as the degree of positivity. The degree of positivity was calculated based on creating a matrix of expression for each cell. Cells were stratified into groups based on whether the probe count for each gene totaled 0–2, 2–4, 4–6, 6–8, and 10–infinity, creating 36 unique cell populations based on the degree of positivity of *CDKN3*⁺ cells, *PRC1*⁺ cells, dual-positivity cells, and dual-negativity cells. Low versus high short Shannon Index scores were based on the median value for each cohort (due to the small sample size), which were 0.486 for LCI and 0.581 for TIGER-LC.

To assess the distances from a *CASP3*⁺ cell to a *CDKN3*⁺*PRC1*⁺ cell, the HALO proximity analysis module was used, which only allowed for the selection of two unique cell populations. For each patient, each distance of a *CASP3*⁺ cell to a nearby *CDKN3*⁺*PRC1*⁺ cell was measured, and the average distance was calculated; therefore, each patient had one value depicted as the overall average distance. Next, patients were stratified based on whether they had an overall average short distance versus long distance, which was based on the median value for each cohort.

Classification of *CASP3*⁺ cell islands and Shannon entropy calculation

To determine first whether there exists a collective density of *CASP3*⁺ (>1 probe copy of *CASP3* per cell was used as the cutoff) in regions of a tumor, density contour maps were generated using R Studio, which performs a two-dimensional kernel density estimation at

subsequent levels. From here, we selected the contour level/line that best reflected the true *CASP3*⁺ cell island and determined the entropy of nearby cells using the *entropy* package from R Studio. All *CASP3*-negative cells were divided into short versus long groups. We assessed the diversity (also referred to as *entropy*) score of *CDKN3*⁺*PRC1*⁺ cells, *CDKN3*⁺ only cells, and *PRC1*⁺ cells within a short or long distance to a *CASP3*⁺ cell island. We calculated the diversity (or entropy) based on these three unique cell populations using the *entropy* package in R. This classification was determined by capturing cells within a distance of 100 arbitrary units using the spatial coordinate map for the short distance group. All other cells classified outside of the distance of 100 were grouped as long distance. Low versus high short Shannon entropy scores were based on the median value for each cohort.

For further details regarding materials and methods, please refer to the Supporting Information.

RESULTS

Selection of heterogeneity markers to model tumor diversity

To identify markers to use for the RNAScope *in situ* hybridization assay, a robust computational approach was used. This method is summarized in the Supporting Information. From this approach, *CDKN3* and *PRC1* were selected. For an apoptotic marker, *CASP3* was selected to measure the apoptotic levels of each tumor sample as its mRNA expression from our RNA-seq data correlates with an apoptotic index we previously calculated (Figure S1B),^[4] and multiple studies have shown it to be a reliable readout of the apoptotic levels in tumor samples.^[4,8,9,10,11,12] We further confirmed that the expression of *CASP3*, *CDKN3*, and *PRC1* is highly variable and tumor-specific in three bulk transcriptome HCC cohorts (Figure S2A–C). To begin the RNAScope assay, positive and negative control probes were stained, to ensure that the sensitivity and specificity of the assay in our patient samples before initiating staining of the markers (Figure S3). The workflow for staining includes using TMAs of paired nontumor and tumor samples in our discovery cohort (LCI), and after undergoing RNAScope staining, each slide was imaged using confocal microscopy and quantified using HALO by Indica Labs (Figure 1A). This experimental workflow was then used again in our validation cohort (TIGER-LC). Single-cell detection of each marker is denoted by individual dots with *CASP3* in green, *CDKN3* in red, and *PRC1* in purple and cell nucleus detection by DAPI staining with HALO software approximating cytoplasm boundary (Figure 1B). The average copies of each marker, *CASP3*, *CDKN3*, and *PRC1*, were quantified in both cohorts and showed highly variable

expression in tumor compared to nontumor samples, indicating varying degrees of apoptotic cell death and heterogeneity, proving that these markers are sufficient to model the diversity of each tumor sample at the single-cell level (Figure 1B). Furthermore, the tissue expression of *CASP3* from the RNAScope assay modestly correlated with our LCI transcriptome RNA-seq data (Figure S4A). On a larger scale, the total percent positivity for each of the markers was also highly abundant and variable in both cohorts (Figure S4B,C). We further validated *CASP3* as a surrogate for cell death by conducting an *in vitro* experiment of treating HuH1 cells, an HCC line, with doxorubicin at varying concentrations to induce different levels of cell death (Figure S5A). We found that as the degree of cell viability decreased (i.e., higher cell death), the *CASP3* mRNA expression of these cells significantly increased (Figure S5B). Furthermore, the protein levels of cleaved *CASP3* increased with increased cell death (Figure S5C), and when tumor samples were stratified by cleaved *CASP3* expression through immunohistochemistry, patients who had a higher immunohistochemistry score had higher levels of *CASP3* positivity in the RNAScope assay (Figure S5D). Thus, the mRNA *CASP3* levels could be used as a sensitive marker and surrogate of cell death. Given these findings, it is evident that single-cell *in situ* hybridization staining of *CASP3*, *CDKN3*, and *PRC1* using the RNAScope platform can recapitulate the diverse and tumor-specific expression in our two liver cancer cohorts and can be used to further understand the tumor and microenvironmental spatial architecture of our patient samples.

Increased apoptotic cell death is associated with increased tumor diversity

In order to assess the heterogeneity level of each tumor sample, a Shannon Index (quantification of entropy) score^[7] based on the percent of cell populations that express *CDKN3*, *PRC1*, both, or neither was computed for each paired tumor and nontumor sample. In both cohorts, tumor samples (LCI, 0.809 [mean] ± 0.832 [SD]; TIGER-LC, 0.702 ± 0.604) displayed a significant increase in diversity (Shannon Index) as well as higher variability compared to nontumor samples (LCI, 0.358 ± 0.310; TIGER-LC, 0.158 ± 0.205), demonstrating that quantification of heterogeneity based on these markers reiterates published literature that diversity can be measured using samples stained with a selected number of markers (Figure 2A).^[7,13,14,15] Moreover, the percent *CASP3* positivity in tumor samples was positively associated with its corresponding Shannon Index in LCI ($R = 0.716$, $p < 0.0001$) as well as in TIGER-LC ($R = 0.708$, $p < 0.0001$; Figure 2B). These findings corroborate our previous work showing that increased apoptotic levels among single cells from single-cell

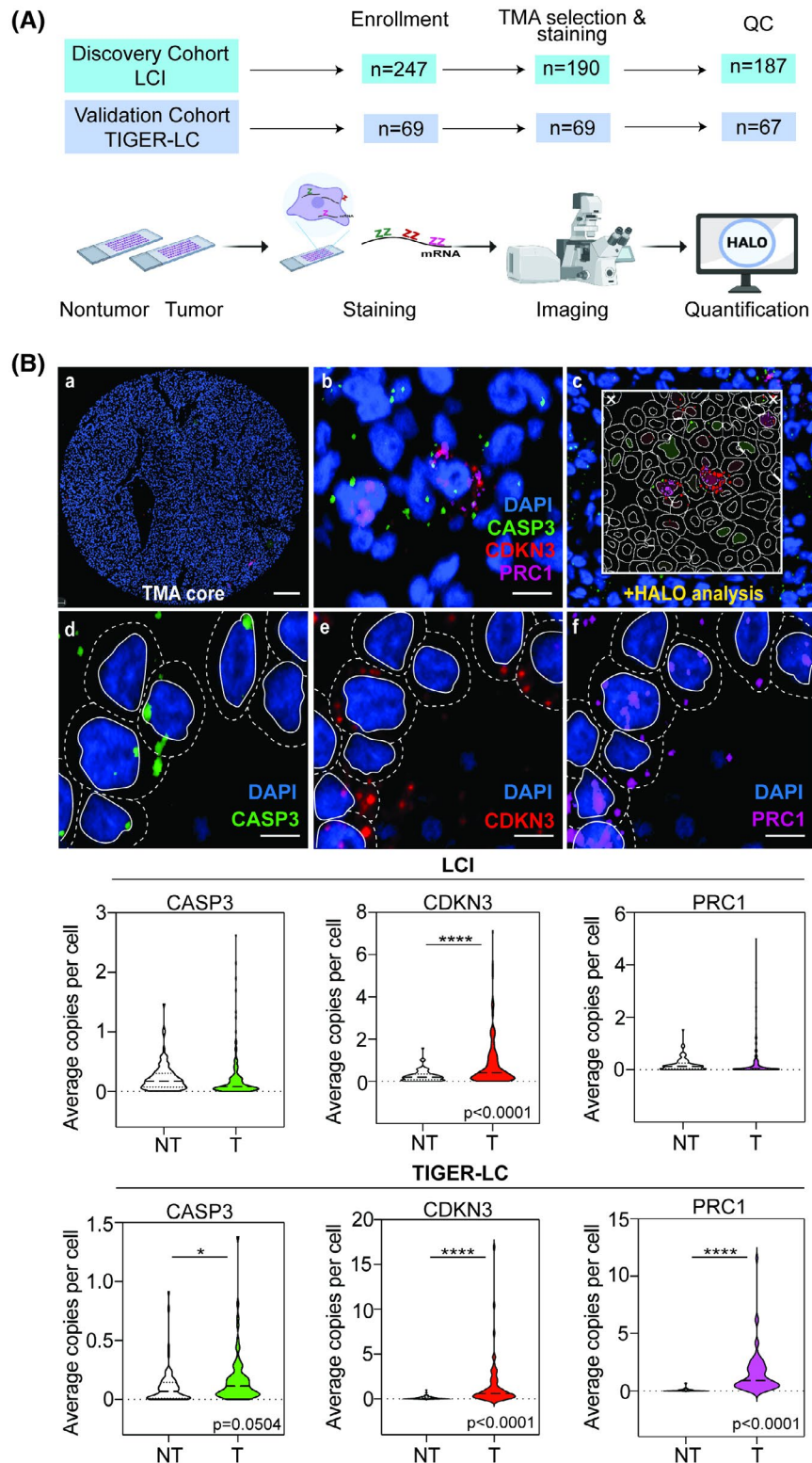


FIGURE 1 Single-cell *in situ* hybridization profiling of HCC tumors from two separate patient cohorts. (A) Workflow of HCC tumor selection, processing, staining, imaging, and computational pathology quantification using HALO software. (B) Top panel: (a) Representative TMA core image, scale bar, 200 μ m. (b) Representative image stained with all markers (DAPI, blue; *CASP3*, green; *CDKN3*, red; *PRC1*, purple). (c) Output image of HALO analysis of single-cell detection (smaller circle indicates nucleus detection, larger circle indicates cytoplasm detection). (d) Single-cell detection of *CASP3* with solid circular outline indicating nucleus detection and dotted circular outline indicating cytoplasm detection. (e) Single-cell detection of *CDKN3* with solid circular outline indicating nucleus detection and dotted circular outline indicating cytoplasm detection. (f) Single-cell detection of *PRC1* with solid circular outline indicating nucleus detection and dotted circular outline indicating cytoplasm detection. Scale bars (d–f), 10 μ m. Bottom panel: Quantification of average copies of *CASP3*, *CDKN3*, and *PRC1* per single cell in our discovery cohort (LCI) and validation cohort (TIGER-LC). All *p* values are reported in the figure. NT, nontumor; QC, quality control; T, tumor

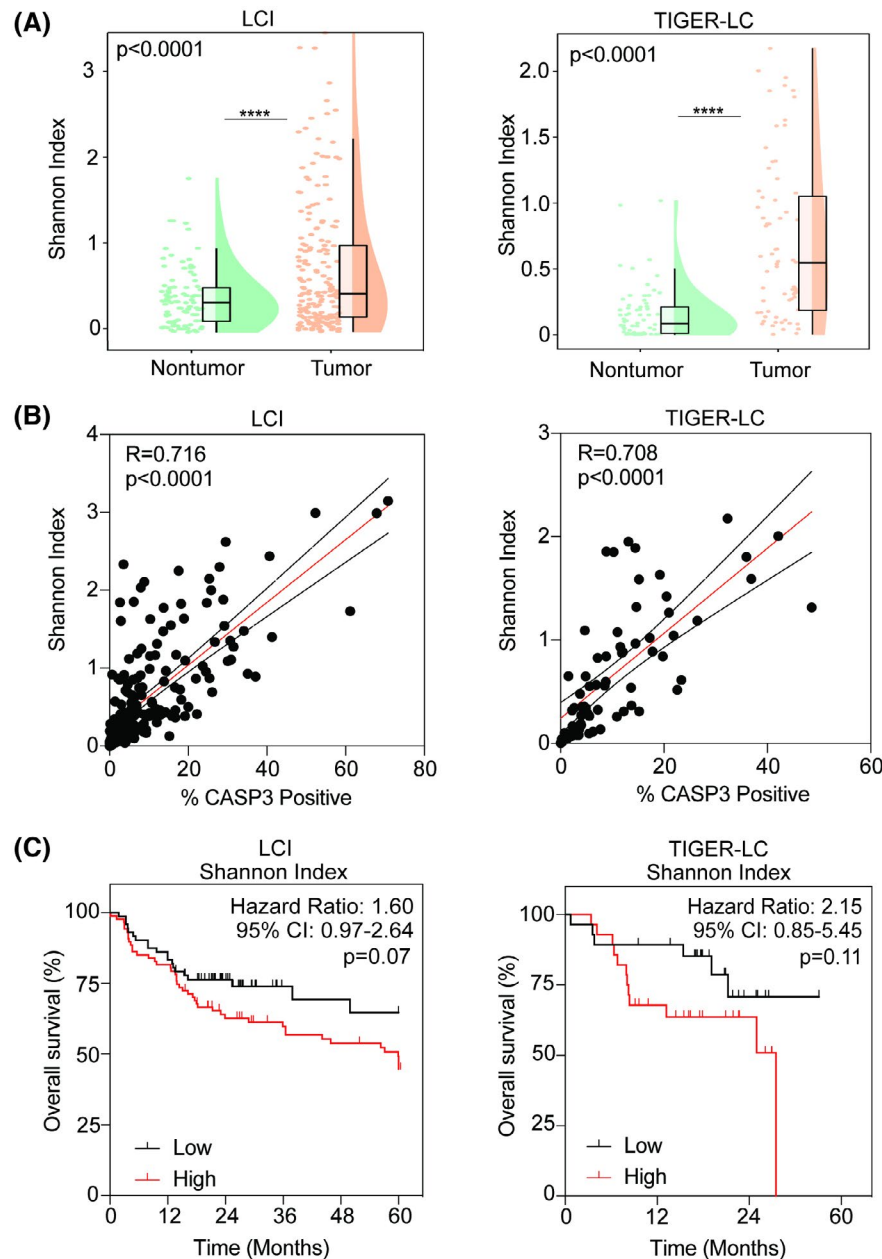


FIGURE 2 Determination of heterogeneity and its association with apoptotic levels and patient outcome. (A) Computed Shannon Index based on *CDKN3* and *PRC1* expression at the single-cell level. (B) Correlation of percent *CASP3* positivity and Shannon Index in HCC tumors. Correlation coefficient and *p* values are based on the Pearson correlation coefficient test. (C) Kaplan-Meier survival analysis of patients with HCC based on high versus low Shannon Index using log-rank *p* value. All *p* values are reported in the figure

RNA-seq data are associated with increased tumor diversity.^[4] Furthermore, to assess whether there is a biological impact of high ITH, patients in each cohort were stratified in high versus low Shannon Indices based on the median value, and their survival data were computed. For the LCI cohort, the HR was numerically higher for high Shannon Index compared to low; however, the results were not statistically significant (HR, 1.60; 95% CI, 0.97–2.64; Figure 2C). Likewise, TIGER-LC patients also displayed a higher HR for high Shannon Index compared to low, but this comparison was not statistically significant (HR, 2.15; 95% CI, 0.85–5.45; Figure 2C).

Together, these data suggest that tumor-specific diversity may be influenced by the degree of apoptotic cell death, which can be related to patient outcome, similar to our previously published findings.^[4]

Tumor diversity is influenced by the spatial context of an apoptotic cell

To determine the impact of apoptotic cell death on the surrounding tumor diversity, spatial analysis was conducted between two distinct cell populations, *CASP3*⁺

cells and $CDKN3^+PRC1^+$ cells (Figure 3A). We investigated the spatial relationship between an apoptotic cell and nearby diverse cell populations by dividing patients into short versus long distances (Figure 3B) and determined the relationship between percentage of $CASP3$ positivity and Shannon Index. Interestingly, patients whose distance of a $CDKN3^+PRC1^+$ double-positive cell to a $CASP3^+$ cell was considered short existed on the high end of the percentage of $CASP3^+$

and Shannon Index spectrum, meaning the shorter the distance, the greater the diversity of the tumor (LCI, $R = 0.712$, $p < 0.0001$; TIGER-LC, $R = 0.533$, $p = 0.0006$; Figure 3B). Those whose distances were longer displayed lower levels of $CASP3$ positivity and lower tumor diversity (LCI, $R = 0.292$, $p = 0.0047$; TIGER-LC, $R = 0.375$, $p = 0.054$; Figure 3B). These observations imply that the diversity of a tumor may be influenced by the degree of apoptotic cell death as

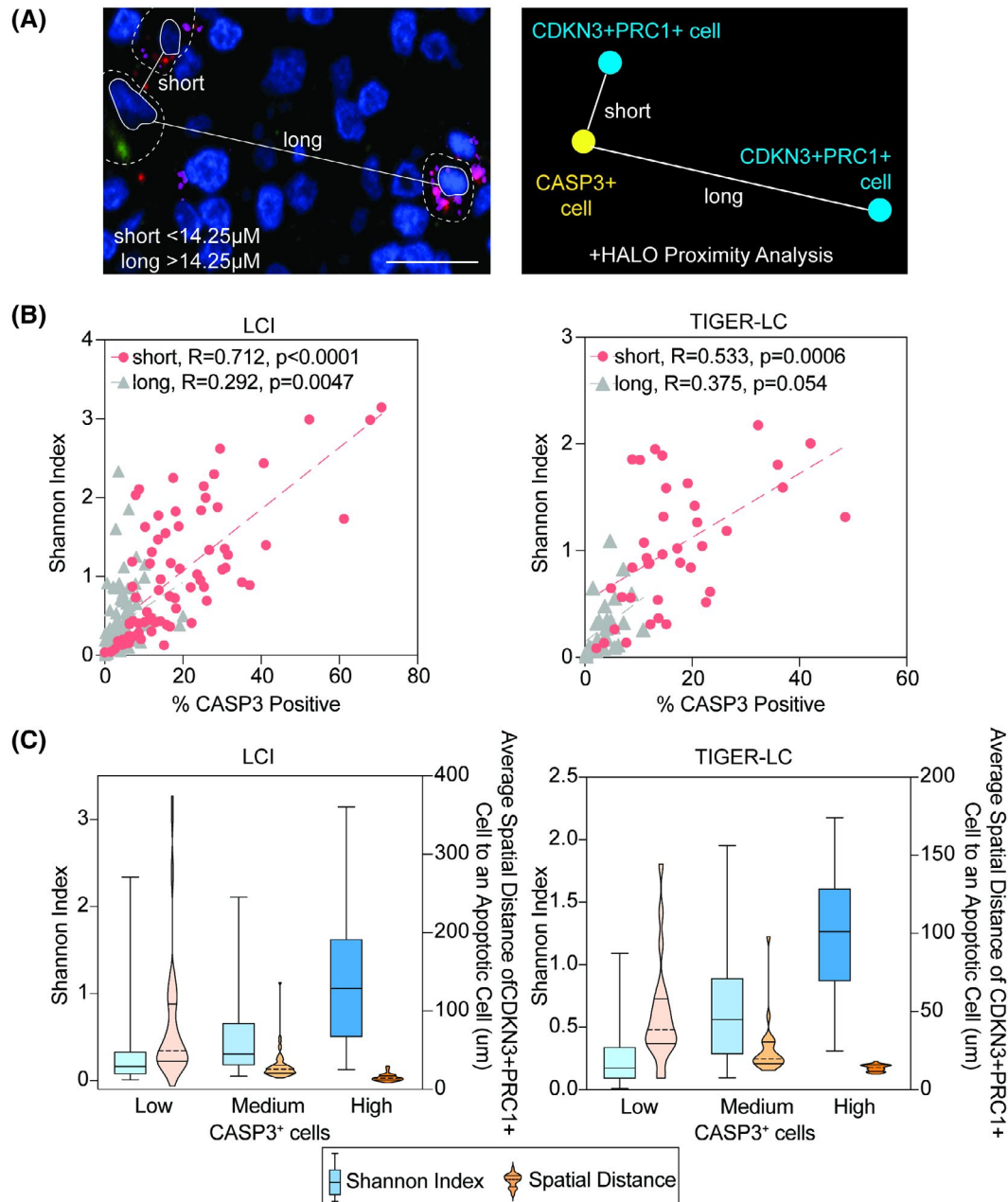


FIGURE 3 Cell death promotes tumor diversity by spatially interacting with its neighboring cells. (A) Representative image and analysis output obtained from HALO of the proximity analysis of a diverse cell ($CDKN3^+PRC1^+$) in blue to an apoptotic cell ($CASP3^+$) in yellow. Each proximity line was classified into either short versus long based on the cutoff of $14.25 \mu\text{m}$. (B) Classification of patients who have higher levels of cell death and diversity are in closer proximity (shorter distance) to a dying cell. (C) Patients stratified based on low, medium, and high levels of cell death exhibit increasing levels of diversity and closer proximity to a diverse microenvironment. Shannon Index depicted in box plots, and spatial distance depicted in violin plots. All p values are reported in the figure

well as the spatial context of an apoptotic cell. Similarly, we divided patients into low, medium, and high levels of *CASP3*⁺ cells based on quartiles and found a stepwise increase in the Shannon Index and a stepwise decrease in the spatial distance of diversity to an apoptotic cell (Figure 3C).

Tumor *CASP3*⁺ cell islands increase nearby heterogeneity

To further investigate the role of apoptosis in promoting nearby tumor diversity, we classified *CASP3*⁺ cell islands based on *CASP3*⁺ cells using density contour mapping. We hypothesized that diversity is the greatest within a close proximity to a collective body of cells classified as a *CASP3*⁺ cell island (Figure 4A). Coordinates for each individual cell were extracted, and density maps of *CASP3* expression were curated for each patient. Interestingly, we found that patients' tumor samples exhibited a collection of *CASP3*⁺ cells to form islands, with each tumor having a unique island architecture distinct from one another (Figure 4B). To assess the diversity near these *CASP3*⁺ cell islands, a Shannon entropy score was determined for cells within a short distance (determined by a contour level of 1 or 2, which was kept constant for each tumor), and all other cells were classified as long distance. We observed significantly higher levels of cell diversity within a short distance to an *CASP3*⁺ cell island for contour level 1 compared to the long distance entropy in both LCI (short, 0.584 ± 0.525 ; long, 0.391 ± 0.386 ; $p = 0.0002$) and TIGER-LC (short, 0.589 ± 0.409 ; long, 0.396 ± 0.324 ; $p = 0.0042$) cohorts (Figure 4C). Furthermore, when the selection of the boundary for the *CASP3*⁺ cell island was changed to contour level 2, we observed significantly similar results between short and long entropies (LCI, short, 0.606 ± 0.548 ; long, 0.421 ± 0.414 ; $p = 0.0006$; TIGER-LC, short, 0.615 ± 0.432 ; long, 0.473 ± 0.350 ; $p = 0.045$) as in contour level 1, showing that this phenomenon is stable across different areas of an island (Figure 4C).

Moreover, patients were divided into low versus high short entropy scores based on the median, and we found that those in the high category for the LCI cohort exhibited a significantly worse overall survival compared to the low category group within the short entropy classification (HR, 2.10; 95% CI, 1.21–3.66; $p = 0.015$; Figure 4D). Likewise, in the TIGER-LC cohort, patients in the high category group displayed significantly worse overall survival versus the low category group within the short entropy classification (HR, 3.09; 95% CI, 1.07–8.93; $p = 0.037$; Figure 4D). Interestingly, when patients were similarly divided into high versus low for the long distance entropy classification, no significant difference in survival was observed (Figure 4D). Because several clinical variables were associated with

HCC prognosis, we further determined whether tumor heterogeneity-associated survival was confounded by underlying clinical conditions. Univariate and multivariate Cox proportional hazards regression analyses were conducted to assess the influence of various clinical variables with the short entropy scores for each cohort (Table S2). A univariate analysis of various clinical variables in the LCI cohort uncovered short entropy, age, alpha-fetoprotein levels, tumor size, and metastasis as significant predictors of survival; and for the TIGER-LC cohort, the variables short entropy, Child-Pugh score, and tumor size were significant predictors of survival. We next performed a multivariate Cox proportional hazards regression analysis comprised of univariate variables with $p < 0.05$ as described above for each cohort and found that the short entropy score was an independent predictor of patient survival (LCI, HR, 3.4; 95% CI, 1.1–10.8, $p = 0.038$; TIGER-LC, HR, 5.5; 95% CI, 1.2–24.0; $p = 0.025$). These results show that regions within a tumor that form *CASP3*⁺ cell islands cause greater diversity in shorter proximity to collective apoptotic cell death versus cells that are farther away and that this phenomenon may be related to patient outcome.

Selective induction of cell death may lead to therapy resistance

To further expand upon our RNAScope findings, we created an *in vitro* model to selectively induce cell death at different levels using CRISPR/Cas9 gene editing in order to assess whether subjecting cells to greater levels of cell death leads to increased heterogeneity of the cell population. We used a tet-on inducible Cas9 plasmid whose expression is activated upon the addition of doxycycline (DOX) and inserted a single-guide RNA (sgRNA) of myeloid cell leukemia 1 (MCL-1; an antiapoptosis gene), knockout of which would promote cell death (Figure 5A). A stable Cas9-expressing Huh1 cell line was created (Figure 5B), and validation of MCL-1 knockout and reduction of cell death at varying multiplicity of infection (MOI) were observed (Figure 5C). To selectively induce different levels of cell death, various concentrations of DOX were added to Huh1 Cas9 cells transduced with the sgRNA virus at an MOI of 2; and concentrations of 0.01, 1.0, and 4.0 $\mu\text{g}/\text{mL}$ mimicked 0%, 50%, and 90% cell death (CD^0 , CD^{50} , CD^{90}), respectively (Figure 5D). Next, the heterogeneity state of cells subjected to CD^0 , CD^{50} , and CD^{90} was assessed by therapeutic induction of doxorubicin. Greater therapy resistance (i.e., lower drug sensitivity) is a common feature illustrated in highly heterogeneous tumor cell populations,^[16-18] and we tested this phenomenon 5 days post-gene knockout of MCL-1 (Figure 5E, left panel). Interestingly, we found that cells subjected to the highest level of cell death (CD^{90}), rather than CD^{50} , had

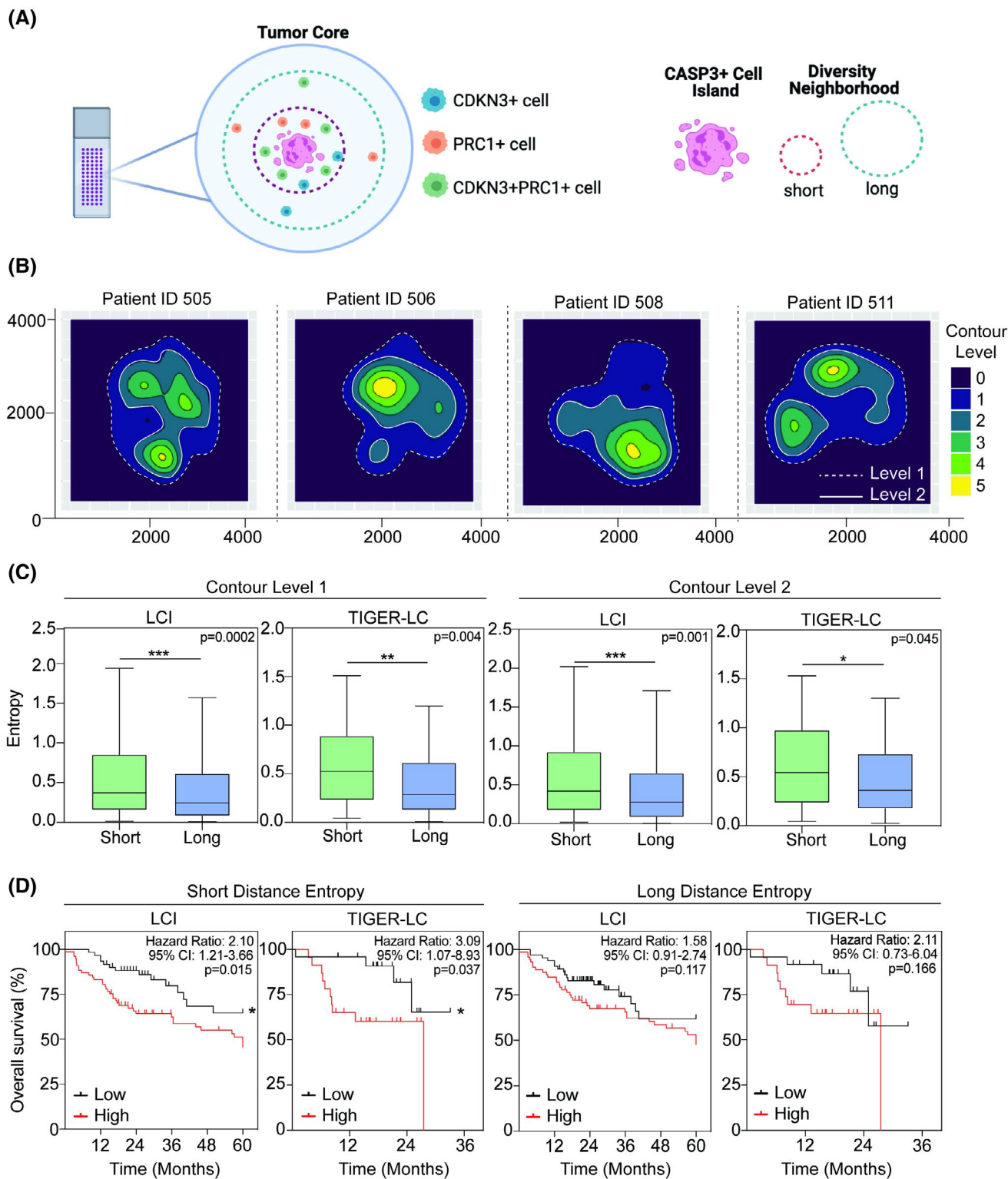


FIGURE 4 Determination of $CASP3^+$ cell islands using spatial coordinates from each patient's tumor and the nearby diversity of short versus long distanced neighborhoods. (A) Proposed model of investigating whether the level of diversity within a tumor is greatest near $CASP3^+$ cell islands. (B) Determination of $CASP3^+$ cell islands among different patients based on $CASP3$ positivity and density separated by varying contour levels. (C) Entropy quantification of short versus long distanced cells to a $CASP3^+$ cell island illustrates higher diversity in the short group versus the long group in both the LCI and TIGER-LC cohorts based on contour levels of either 1 or 2. $p < 0.05$, $**p < 0.01$, $***p < 0.001$. (D) Kaplan-Meier survival analysis of patients with HCC based on high versus low short distanced Shannon Entropy score and long distanced Shannon Entropy score using log-rank p value. All p values are reported in the figure

a significantly reduced sensitivity to doxorubicin, which may infer that a higher degree of cell death is needed to promote a more aggressive phenotype (Figure 5E, right panel). Subsequently, when more time was given to the cells subjected to CD^0 , CD^{50} , and CD^{90} to recover and then treated with doxorubicin for 48 h or placed in a hypoxic chamber for 48 h (Figure 5F), over time the rate of proliferation in the CD^{90} group increased faster (Figure 5G), and the cells survived in hypoxic conditions (Figure 5H). Similar results were obtained in another HCC cell line, Hep3B (Figure S6). Together, these results illustrate in a controlled setting that induction of higher levels of cell death leads to increased therapy resistance and survival in hypoxic conditions, which can be indicative of the heterogeneity level of the tumor cell population.

DISCUSSION

In this study, we sought to determine if there is a direct link between apoptotic cell death and diversity using a multiplex fluorescence-based assay that can measure selected markers at the single-cell level. We used a single cell–based *in situ* hybridization assay in paired tumor and nontumor samples from patients with HCC. Furthermore, we show that apoptotic cell death can be linked to tumor heterogeneity using various mathematical modeling data obtained from stained tumor sections. After appropriate quality controls and optimization, we were able to successfully obtain single cell–level expression data of three markers, *CASP3*, *CDKN3*, and *PRC1*, to use for further characterization. We show that as the level of apoptotic cell death increases in a tumor, the degree of diversity measured by a Shannon Index increases. To further examine whether apoptotic cell death can be associated with tumor diversity, we measured the spatial distance of our heterogeneity markers to an apoptotic cell. We found that tumors with a high degree of apoptotic cell death and high Shannon Index exhibited shorter distances of a *CDKN3*^{+*PRC1*⁺ cell to a *CASP3*⁺ cell. Next, we wanted to determine if an apoptotic cell works alone or collectively as an island to promote the greatest diversity nearby and found that there are distinct regions within a tumor where *CASP3*⁺ cells collectively reside. Interestingly, we found that the highest level of diversity was near regions of densely populated apoptotic cells, or what we refer to as “islands,” and that this phenomenon was associated with survival. Through recent research observations, we have come to appreciate tumor heterogeneity as an intrinsic mechanism of tumor cell survival and evolution and not a random and chaotic event. It is plausible that one way a tumor can further promote heterogeneity so that therapies will not eliminate it is through its own self-destructive mechanisms such as collective apoptosis in the form of islands. These islands can release nutrients}

into the microenvironment and create space for future minor clones to expand, thus increasing the propensity of tumor cells to acquire further heterogeneity to nearby surroundings. Our *in vitro* experimental models under controlled levels of cell death linked to chemotherapy resistance are consistent with this hypothesis.

We have long viewed cancer cell death as the ultimate goal in achieving remission and favorable therapeutic outcomes. However, increasing evidence has shed light on the oncogenic effects of cell death, specifically apoptosis. Various mechanisms have been proposed to elucidate how apoptosis may be protumorigenic instead of antitumorigenic. These include growth factors that are released from apoptotic bodies that can promote cancer stem cell proliferation and immune silencing, selection of treatment-resistant cancer clones causing tumor repopulation, and finally crosstalk between an apoptotic cell and the microenvironment that can lead to proangiogenic proliferation, trophic support, and tumor immune escape.^[19] All of these mechanisms can allow tumors to continue to evolve and maintain their heterogeneous state as diversity intrinsically ensures their continued survival. Just like any other species that promotes various traits within their population, cancer cells use the same phenomenon to evolve through time. While it may seem paradoxical to associate increased cell death with greater tumor diversity and ultimately worse patient outcome, these findings show that a potential mechanism to cause tumor heterogeneity can be related to the removal of major clones in a tumor ecosystem by apoptosis. This scenario can provide the necessary room for minor clones that did not make up the majority of the tumor and were not eliminated by therapy to repopulate the tumor region and promote further diversity. This phenomenon is commonly termed *competitive release* as therapy selects for the resistance clones, thus making the tumor more difficult to treat further along the treatment course.^[20,21] Another possible implication of how cell death in the form of apoptosis can lead to increased diversity is that apoptotic bodies that are released into the microenvironment can fuel the proliferation and survival of other cell types nearby and thus continue to create a diverse tumor population.^[22-24]

While there have been mechanisms proposed that may cause tumor heterogeneity such as genomic instability, inefficient DNA repair machinery, mutational burden, and impaired immune response,^[25-28] one that often gets overlooked is induction of therapy. It has long been known that cancers, especially in late stages, do not respond favorably to remission. While there are many reasons for this, one that is a common phenomenon that can be seen in all solid cancer types is the selection of resistant clones within a tumor through elimination of the sensitive clones by induction of molecularly targeted therapy.^[29-34] Thus, destruction or death of a selected group of cancer cells within a

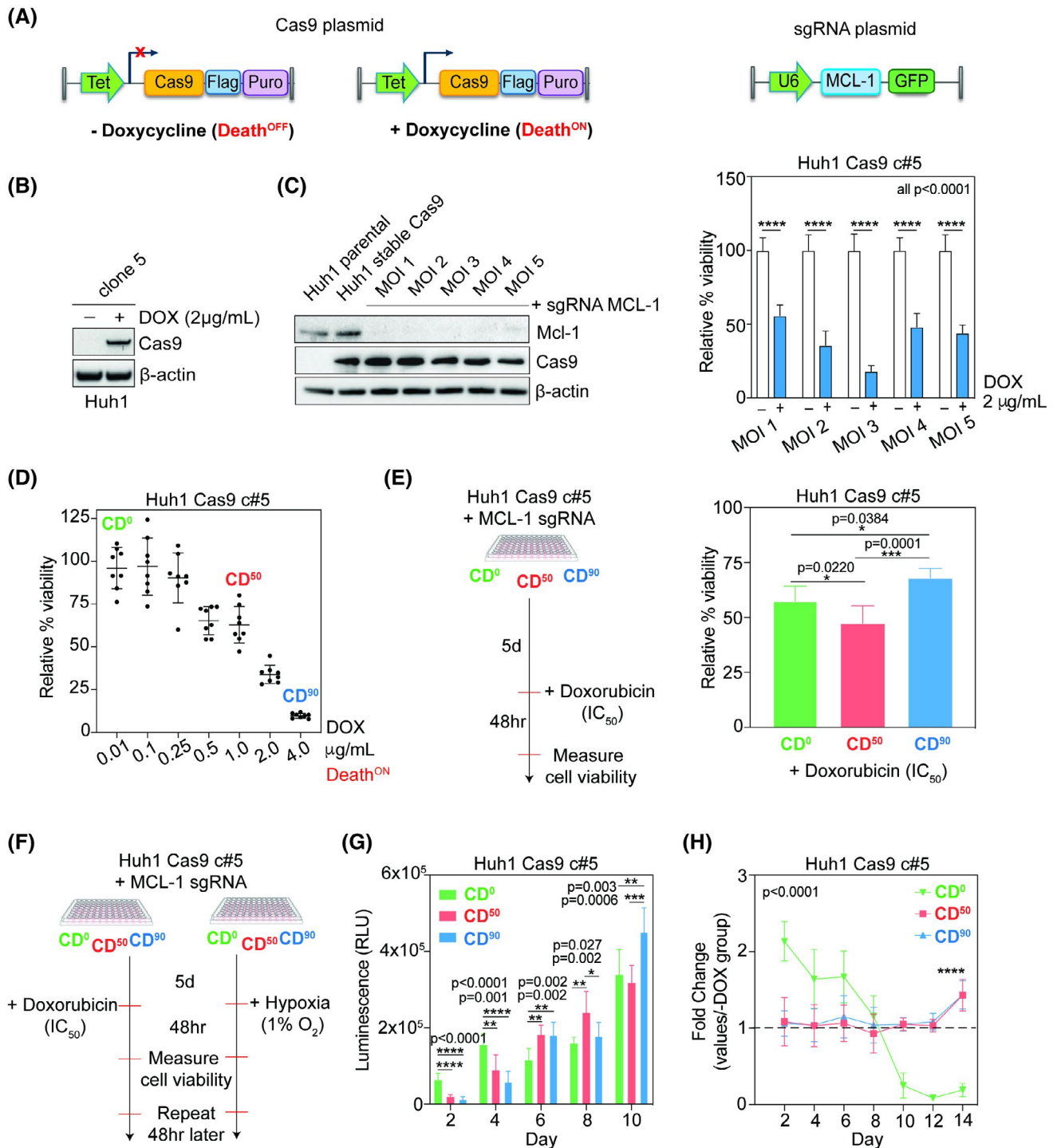


FIGURE 5 Selective induction of cell death using CRISPR/Cas9 to measure drug sensitivity and heterogeneity of Huh1 cells. (A) (Left and middle panels) Illustration of a Cas9 plasmid whose expression is turned on upon the addition of DOX. (Right panel) Illustration of an sgRNA plasmid with a target sequence for the MCL-1 gene inserted and tagged with green fluorescent protein. (B) Screening of single clones isolated from Huh1 cells that were transduced with a lentivirus packaged with the Cas9 plasmid to determine which clone successfully expresses Cas9 to use for downstream functional assays. (C) (Left panel) MCL-1 gene knockout validation. (Right panel) Optimization of the MOI for the MCL-1 sgRNA lentivirus transduced with stable Huh1 Cas9 cells. (D) Induction of varying levels of cell death controlled by the amount of DOX added to stable Huh1 Cas9 cells. (E) (Left panel) Workflow of cells undergoing various levels of cell death for 5 days, then treated with doxorubicin for 48 h to test drug sensitivity. (Right panel) Measuring therapy sensitivity as an output of cellular heterogeneity by treatment with doxorubicin (48 h) from cells that were subjected to varying levels of cell death (10%, 50%, 90%). (F) Workflow of cells undergoing various levels of cell death for 5 days, then treated with doxorubicin for 48 h or placed in a hypoxic chamber for 48 h and repeated until day 10 or 14 from initial cell death induction. (G) Measuring doxorubicin sensitivity at various time points as cells recovered from their initial induction of cell death (0%, 50%, 90%). For each time point, cells were treated with doxorubicin for 48 h, but at each consecutive time point after the previous one, cells had a longer time to recover from initial cell death. (H) Measurement of cellular viability of cells that underwent varying levels of death and were placed in a hypoxic chamber at 1% O₂ for 48 h, repeated until day 14. All p values are reported in the figure. GFP, green fluorescent protein; IC₅₀, 50% inhibition concentration; RLU, relative light units

tumor can make tumors more heterogeneous as the resistance clones that get left behind can repopulate the vacant niche through expansion of minor clones with diverse characteristics.

On the contrary, one mechanism of tumor heterogeneity that has not yet been proposed is the collective assembly of apoptotic cells in a tumor to form a *CASP3*⁺ cell island to elicit diversity from its nearby surroundings. We believe cancer cells may behave in a collective and symbiotic manner such as the creation of “apoptotic islands” within a tumor that promote cell death in certain regions to further its diversity and microenvironmental heterogeneity, much like how cooperativity and symbiosis have long been observed in organismal species as mechanisms for survival.^[35,36]

The findings of this study highlight critical observations that can be made when integrating the spatial information with transcriptomic profiles of individual cells. Here, we propose that cell death is not a random event but a coordinated effort among multiple cancer cells to form dense, *CASP3*⁺ cell islands that can cause greater local heterogeneity than if each cell were to work alone. Overall, our study shows not only that cancer cell death can be related to tumor heterogeneity but that there is also an organized coordinated effort among cancer cells to collectively induce apoptosis in order to maximize nearby diversity. Therefore, we must begin to incorporate our understanding of the spatial dynamics that make up cells within a tumor to design better therapeutic options for patients with highly aggressive and treatment-resistant cancers.

ACKNOWLEDGMENT

We thank members of the Wang Lab/Liver Carcinogenesis Section for thoughtful and critical discussions; Michael Kruhlak, Langston Lim, and Andy Tran of the Confocal Microscopy Core Facility within the Center for Cancer Research at the National Cancer Institute; and the patients whose contributions led us to conduct this study. This work was supported by grants Z01 BC 010877 and Z01 BC 010876 from the intramural research program of the Center for Cancer Research, National Cancer Institute (Bethesda, MD, USA).

CONFLICT OF INTEREST

The authors declare no competing interests.

AUTHOR CONTRIBUTIONS

Subreen A. Khatib and Xin Wei Wang developed the study concept. Subreen A. Khatib and Lichun Ma performed computational analysis. Subreen A. Khatib, Hien Dang, Marshonna Forgues, and Joon-Yong Chung conducted experiments. Kris Ylaya performed TMA construction. Stephen M. Hewitt performed TMA design, evaluation, and data interpretation. Jittporn Chaisaingmongkol and Mathuros Rucchirawat

provided tissue samples. Subreen A. Khatib acquired imaging data and performed quantitative analysis. Subreen A. Khatib and Xin Wei Wang wrote the manuscript. All authors read, edited, and approved the manuscript.

ORCID

Joon-Yong Chung  <https://orcid.org/0000-0001-5041-5982>

Xin Wei Wang  <https://orcid.org/0000-0001-9735-606X>

REFERENCES

1. Siegel RL, Miller KD, Jemal A. Cancer statistics, 2020. *CA Cancer J Clin.* 2020;70:7–30.
2. Dasgupta P, Henshaw C, Youlden DR, Clark PJ, Aitken JF, Baade PD. Global trends in incidence rates of primary adult liver cancers: a systematic review and meta-analysis. *Front Oncol.* 2020;10:171–1.
3. Chaisaingmongkol J, Budhu A, Dang H, Rabibhadana S, Pupacdi B, Kwon SM, et al. Common molecular subtypes among Asian hepatocellular carcinoma and cholangiocarcinoma. *Cancer Cell.* 2017;32:57–70.e3.
4. Khatib S, Pomyen Y, Dang H, Wang XW. Understanding the cause and consequence of tumor heterogeneity. *Trends Cancer.* 2020;6:267–71.
5. Roessler S, Jia H-L, Budhu A, Forgues M, Ye Q-H, Lee J-S, et al. A unique metastasis gene signature enables prediction of tumor relapse in early-stage hepatocellular carcinoma patients. *Cancer Res.* 2010;70:10202–12.
6. Ma L, Hernandez MO, Zhao Y, Mehta M, Tran B, Kelly M, et al. Tumor cell biodiversity drives microenvironmental reprogramming in liver cancer. *Cancer Cell.* 2019;36:418–30.e6.
7. Janiszewska M, Liu L, Almendro V, Kuang Y, Paweletz C, Sakr RA, et al. In situ single-cell analysis identifies heterogeneity for PIK3CA mutation and HER2 amplification in HER2-positive breast cancer. *Nat Genet.* 2015;47:1212–9.
8. Yan F, He Q, Hu X, Li W, Wei KE, Li LI, et al. Direct regulation of caspase-3 by the transcription factor AP-2 α is involved in aspirin-induced apoptosis in MDA-MB-453 breast cancer cells. *Mol Med Rep.* 2013;7:909–14.
9. O'Donovan N, Crown J, Stunell H, Hill ADK, McDermott E, O'Higgins N, et al. Caspase 3 in breast cancer. *Clin Cancer Res.* 2003;9:738–42.
10. Ho Y-T, Lu C-C, Yang J-S, Chiang J-H, Li T-C, Ip S-W, et al. Berberine induced apoptosis promoting the expression of caspase-8, -9 and -3, apoptosis-inducing factor and endonuclease G in SCC-4 human tongue squamous carcinoma cancer cells. *Anticancer Res.* 2009;29:4063–70.
11. Omezzine A, Mauduit C, Tabone E, Nabli N, Bouslama A, Benahmed M. Caspase-3 and -6 expression and activation are targeted by hormone action in the rat ventral prostate during the apoptotic cell death process. *Biol Reprod.* 2003;69:752–60.
12. Jha K, Shukla M, Kumar M, Shukla VK, Pandey M. Expression of caspase 3 and inhibition of apoptosis lowers survival in breast cancer. *World J Surg Med Radiat Oncol.* 2017;9:7–16.
13. Chung YR, Kim HJ, Kim YA, Chang MS, Hwang K-T, Park SY. Diversity index as a novel prognostic factor in breast cancer. *Oncotarget.* 2017;8:97114–26.
14. Park SY, Gönen M, Kim HJ, Michor F, Polyak K. Cellular and genetic diversity in the progression of in situ human breast carcinomas to an invasive phenotype. *J Clin Invest.* 2010;120:636–44.
15. Almendro V, Kim HJ, Cheng Y-K, Gönen M, Itzkovitz S, Argani P, et al. Genetic and phenotypic diversity in breast tumor metastases. *Cancer Res.* 2014;74:1338–48.

16. Zhao B, Hemann MT, Lauffenburger DA. Intratumor heterogeneity alters most effective drugs in designed combinations. *Proc Natl Acad Sci U S A*. 2014;111:10773–8.
17. Dagogo-Jack I, Shaw AT. Tumour heterogeneity and resistance to cancer therapies. *Nat Rev Clin Oncol*. 2018;15:81–94.
18. Wu D, Wang DC, Cheng Y, Qian M, Zhang M, Shen Q, et al. Roles of tumor heterogeneity in the development of drug resistance: a call for precision therapy. *Semin Cancer Biol*. 2017;42:13–9.
19. Ichim G, Tait SW. A fate worse than death: apoptosis as an oncogenic process. *Nat Rev Cancer*. 2016;16:539–48.
20. Andor N, Graham TA, Jansen M, Xia LC, Aktipis CA, Petritsch C, et al. Pan-cancer analysis of the extent and consequences of intratumor heterogeneity. *Nat Med*. 2016;22:105–13.
21. Elinav E, Nowarski R, Thaiss CA, Hu B, Jin C, Flavell RA. Inflammation-induced cancer: crosstalk between tumours, immune cells and microorganisms. *Nat Rev Cancer*. 2013;13:759–71.
22. Brock CK, Wallin ST, Ruiz OE, Samms KM, Mandal A, Sumner EA, et al. Stem cell proliferation is induced by apoptotic bodies from dying cells during epithelial tissue maintenance. *Nat Commun*. 2019;10:1044.
23. Ryoo HD, Bergmann A. The role of apoptosis-induced proliferation for regeneration and cancer. *Cold Spring Harb Perspect Biol*. 2012;4:a008797.
24. Labi V, Erlacher M. How cell death shapes cancer. *Cell Death Dis*. 2015;6:e1675.
25. Bakhom SF, Landau DA. Chromosomal instability as a driver of tumor heterogeneity and evolution. *Cold Spring Harb Perspect Med*. 2017;7:a029611.
26. von Loga K, Woolston A, Punta M, Barber LJ, Griffiths B, Semiannikova M, et al. Extreme intratumour heterogeneity and driver evolution in mismatch repair deficient gastroesophageal cancer. *Nat Commun*. 2020;11:139.
27. Sung J-Y, Shin H-T, Sohn K-A, Shin S-Y, Park W-Y, Joung J-G. Assessment of intratumoral heterogeneity with mutations and gene expression profiles. *PLoS One*. 2019;14:e0219682.
28. McDonald K-A, Kawaguchi T, Qi Q, Peng X, Asaoka M, Young J, et al. Tumor heterogeneity correlates with less immune response and worse survival in breast cancer patients. *Ann Surg Oncol*. 2019;26:2191–9.
29. McGranahan N, Swanton C. Clonal heterogeneity and tumor evolution: past, present, and the future. *Cell*. 2017;168:613–28.
30. Burrell RA, Swanton C. Tumour heterogeneity and the evolution of polyclonal drug resistance. *Mol Oncol*. 2014;8:1095–111.
31. Williams JB, Li S, Higgs EF, Cabanov A, Wang X, Huang H, et al. Tumor heterogeneity and clonal cooperation influence the immune selection of IFN- γ -signaling mutant cancer cells. *Nat Commun*. 2020;11:602.
32. Seth S, Li C-Y, Ho I-L, Corti D, Loponte S, Sapio L, et al. Pre-existing functional heterogeneity of tumorigenic compartment as the origin of chemoresistance in pancreatic tumors. *Cell Rep*. 2019;26:1518–32.e9.
33. Ramón y Cajal S, Sesé M, Capdevila C, Aasen T, De Mattos-Arruda L, Díaz-Cano SJ, et al. Clinical implications of intratumor heterogeneity: challenges and opportunities. *J Mol Med*. 2020;98:161–77.
34. Venkatesan S, Swanton C. Tumor evolutionary principles: how intratumor heterogeneity influences cancer treatment and outcome. *Am Soc Clin Oncol Educ Book*. 2016;35:e141–9.
35. Feeney WE, Medina I, Somveille M, Heinsohn R, Hall ML, Mulder RA, et al. Brood parasitism and the evolution of cooperative breeding in birds. *Science*. 2013;342:1506–8.
36. Hemelrijk C, Reid D, Hildenbrandt H, Padding J. The increased efficiency of fish swimming in a school. *Fish Fish*. 2015;16:511–21.

SUPPORTING INFORMATION

Additional supporting information may be found in the online version of the article at the publisher's website.

How to cite this article: Khatib SA, Ma L, Dang H, Forgues M, Chung J-Y, Ylaya K, et al. Single-cell biology uncovers apoptotic cell death and its spatial organization as a potential modifier of tumor diversity in HCC. *Hepatology*. 2022;00:1–13. <https://doi.org/10.1002/hep.32345>